

Characterization and fabrication of silver nanoparticles prepared by multiple methods and their antibacterial and antifungal effects

Sabah Ali Khadhir

Ministry of Education / General Directorate of Education Diyala

Email: sciphydr222307@nodiyala.edu.iq

Abstract

Various methods have been developed to produce silver nanoparticles with the aim of obtaining pollutant-free water. There is significant interest in developing production processes that are environmentally friendly and reducing the use of antibiotics. Chemical preparation methods utilizing various silver precipitants and physical methods have emerged to enhance the effectiveness of silver nanoparticles against small organisms, demonstrating potential biological applications in combating bacteria and fungi. Understanding the impact of silver placement on filters and its influence on bacteria, particularly *Escherichia coli*, a common bacterium, is crucial due to its association with other pollutants. This study explores the production of silver nanoparticles through two distinct biosynthesis methods. The manufactured silver is then utilized as an inhibitor for isolated bacteria and fungi, with subsequent separation of the silver nanoparticles prepared using both techniques. Various tests such as UV, FTIR, EDX, and AFM were conducted to analyze the properties of the nanoparticles. Additionally, changes in color from pale yellow to dark yellow were observed in the mixture of powder and colloidal liquid.

Keywords: Antimicrobial activity, *Escherichia coli*, silver nanoparticles, UV-vis spectrophotometry, nanoparticles, AFM.

1-Introduction

Nanotechnology has significantly transformed the field of materials science, particularly in the design and manufacturing processes, by manipulating particles ranging from 1-100 nanometers. This technology shows great potential for creating new products with medical applications, including early detection and treatment. Silver has been selected for its antimicrobial properties, acting both internally and externally [1,2]. Consequently, metal nanoparticles have garnered significant research interest due to their various advantageous applications in fields such as biomedicine, drug delivery, agriculture, and textiles. They can be synthesized using multiple chemical and physical methods. Notably, nanoparticles are gaining attention as a rapid, cost-effective, environmentally friendly method for human therapeutic use. In a recent study, silver nanoparticles were synthesized through a bacterium that was isolated for this purpose. Their antibacterial activity against environmental and pathogenic bacteria as well as fungi was evaluated [3]. Silver metal and its ions exhibit antibacterial properties against both Gram-positive and Gram-negative bacteria. The mechanism of their antibacterial activity involves interactions between the ions and thiol groups in enzymes and proteins essential for the respiration and substance transport across the cell membrane in these bacteria. Furthermore, the binding of silver ions to the bacterial cell membrane leads to bacterial death [4]. The human physiological system has the ability to convert silver metals into silver ions for interaction with bacterial cells. Elevated levels of silver ions can cause harm to normal human cells, leading to cytotoxic effects. Silver nitrate can be transformed into silver nanoparticles through the use of glucose as a reducing agent and polyvinyl alcohol as a suitable host material. This reduction process is commonly employed in biomedical and semiconductor applications due to its high thermal stability and resistance to chemical reactions [11-14]. Numerous in vitro studies have been carried out to investigate the cytotoxicity of silver nanoparticles and their impact on oxidative stress. Recent developments have explored the use of natural polymers such as cellulose, chitin, and chitosan for coating silver nanoparticles in order to mitigate their cytotoxic effects. The primary aim of this research is to synthesize silver nanoparticles using a green approach involving glucose and polyvinyl alcohol, with the goal of minimizing their cytotoxicity compared to chemical reduction methods, for application in large-scale medical textiles [5]. Laser ablation technology offers a distinctive approach for producing metal nanoparticles. This technique involves using a high-powered laser to ablate a metal plate in a liquid, resulting

in the formation of nanoparticles. The unique properties of nanoparticles created through laser ablation cannot be replicated by other methods, such as chemical processes. Key factors in the production of metal nanoparticles through laser ablation include energy, wavelength, repetition rate of the laser, ablation time, and absorption of the aqueous solution. Laser ablation provides a straightforward means of manufacturing metal nanoparticles without the need for surfactants or chemicals [6]. In recent decades, silver has been utilized as a medical remedy. Silver particles have shown diverse potential in catalysis, optics, electronics, and other domains due to their unique size, optical dependency, and electrical and magnetic properties. The predominant applications of silver nanoparticles are found in antibacterial and antifungal agents, biotechnology and engineering, textile engineering, water purification, and consumer products containing silver. Efforts are being made to integrate various silver nanoparticles into a wide array of uses. A substance known as "Nano silver," incorporating dispersed silver particles on household appliance surfaces, is manufactured and marketed for medical device purposes by the company [3].

2-EXPERIMENTAL WORK

The prepared high purity nanosilver powder was taken as sample 1, and tested for comparison with silver produced from silver nitrate, an AgNO_3 compound with a purity of 99.9% and a molecular weight of 169.87. Silver nitrate, manufactured in Belgium, was dissolved in non-ionic distilled water with continuous rotation and heated to 60 °C before adding HCl acid to the solution. The pure silver settled at the bottom of the vessel, was dried at 150 °C, ground, and then burned at 500 °C. In contrast, for sample 2, NaCl salt was added to the dissolved silver nitrate solution with rotation until the silver nitrate precipitated in powder form and was considered sample 3. The color of the resulting colloidal solution varied depending on the concentration of the solution containing the silver nanoparticles and their concentration, showing a range from pale yellow to dark yellow. Sample 4 was prepared by ablation of a silver plate with a purity of 99% by laser ablation with an energy of 750 mJ, a number of strokes of 3000, and a frequency of 1 Hz, and sample 5 was prepared by ablation with an energy of 650 mJ. Sample 6 included the method of dissolving the silver plate in HNO_3 acid to produce silver nitrate.

2.1. Characterization of silver nanoparticles [Ag NPs]

The samples underwent analysis using ultraviolet (UV) and ultraviolet-infrared (FTIR) spectroscopy to assess the sensitivity of silver colloids. This is because AgNPs exhibit intense absorption peaks resulting from surface Plasmon excitation and collective excitation of conductive electrons in the metal. Additionally, atomic force microscopy (AFM) was utilized to measure the sample's volumetric rate, and energy dispersive spectroscopy (EDAX/DX4) was employed to determine the silver content percentages within the samples. The samples were analyzed in biological studies to evaluate their efficacy against two types of bacteria commonly found in drinking water, namely negative and positive. Additionally, the samples were also tested for their inhibitory effects on two categories of fungi, strong and weak. Silver demonstrated its effectiveness in inhibiting both bacteria and fungi, with the inhibition zones being determined by drilling a small circle in the center of pre-prepared agar. The inhibitor's effectiveness was assessed through dilution testing at various concentrations, allowing for the determination of inhibition zone diameters using a ruler. Powdered samples were diluted to three different concentrations, while colloidal liquids were directly applied to the samples and 0.01 was extracted using a fine pipette for analysis.

3-RESULTS AND DISCUSSION

3.1.UV-visible spectrum results

The findings of this study indicated that silver nanoparticles fall within the range of 300 to 800 nanometers. The UV absorption spectrum of silver nanoparticles was observed to be within this range [7], as depicted in Figure.

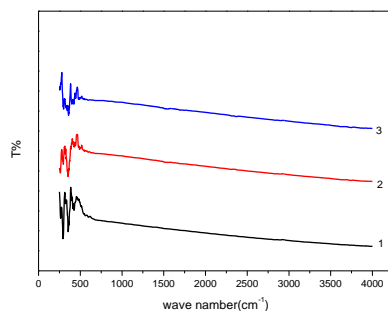


Fig. 1 . UV-vis spectra of silver nanoparticles prepared by chemical precipitation.

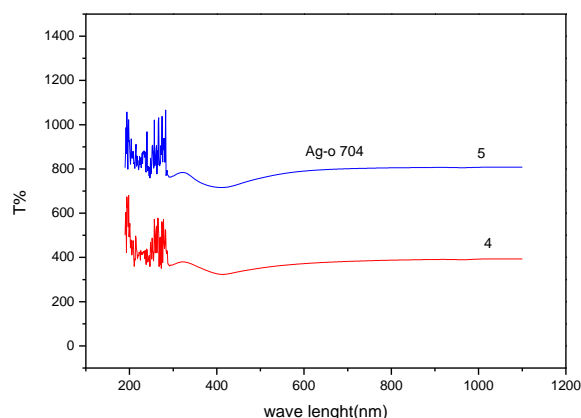


Fig . 2 . UV-vis spectra of silver nanoparticles ablated by laser at different energies.

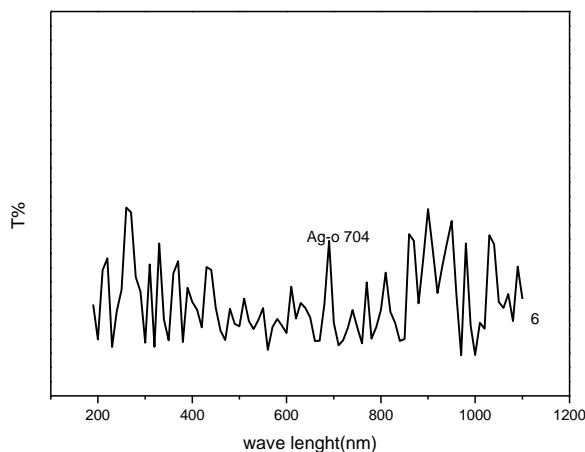


Fig. 3 . UV-Vis spectra of silver nanoparticles for silver plate dissolution method with HNO₃ acid .

Preparation of silver nanoparticles in both organic and inorganic solutions is a topic of interest due to the biological, thermal, optical, and electrical properties exhibited by these particles. The synthesis of physical silver nanoparticles and laser ablation of silver plate offers an environmentally friendly method for preparing silver nanoparticles in aqueous solutions. These nanoparticles exhibit localized surface plasmon resonance or plasmon band when exposed to laser beams at wavelengths of 355, 532, and 1064 nm. Additionally, the absorption of colloidal silver is more noticeable at shorter wavelengths, particularly in the range of 400 to

600 nm as reported by previous studies [8, 9].

3.2. Fourier transform infrared spectroscopy [FTIR] results

The presence of silver nanoparticles is indicated by a broad absorption band at 430 nm in the figure [4]. Additionally, the clear band at 3380 cm is attributed to water adsorbed on the silver nanoparticles as observed in reference [10].

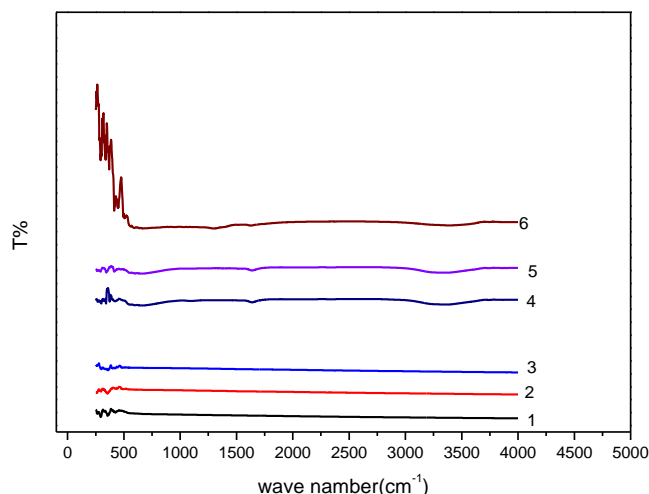


Fig. 4 . shows the FTIR spectra of Nano silver samples prepared by methods different.

3.3 .EDS Results

The EDX verification results indicated that the silver content in Figure 9 of the initial sample was 98.09%, while in the second sample (Figures 5, 6, 7, 8) it was measured at 58.07%. The third sample showed a silver percentage of 49.43%, a silver percentage of 24.05%. These variations are attributed to differences in the preparation conditions, as mentioned in reference [11]. The concentration levels were found to be influenced by the specific methods used for preparation.

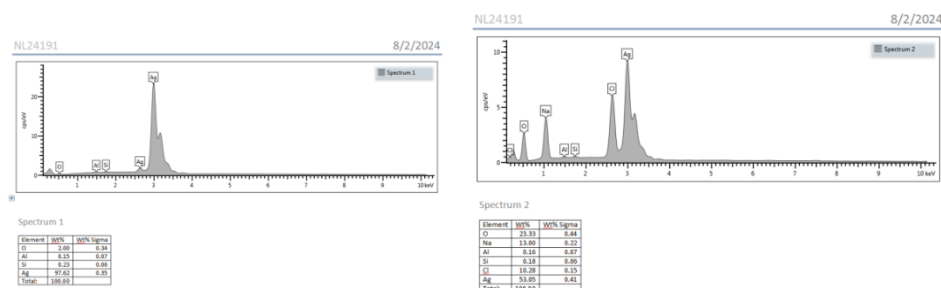


Fig. 5 . EDX spectra analysis of A- sample 1 and B- sample 2 .

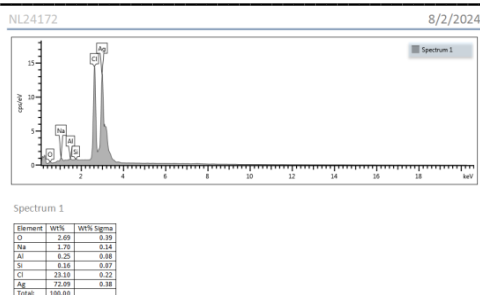
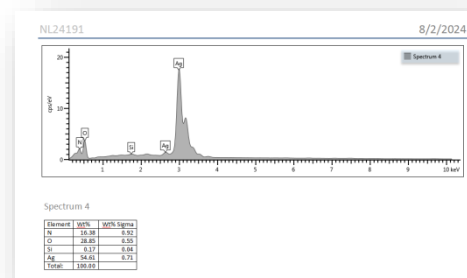
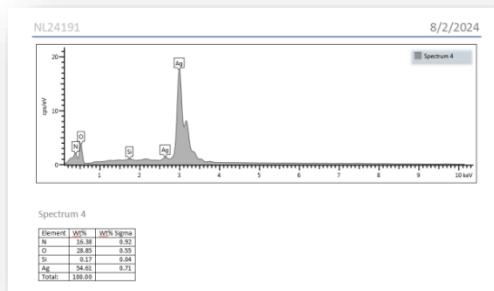


Fig. 6 . EDX spectra analysis of sample 3 .



A-

B-

Fig. 7 . EDX spectra analysis of A-sample 4 B- sample 5.

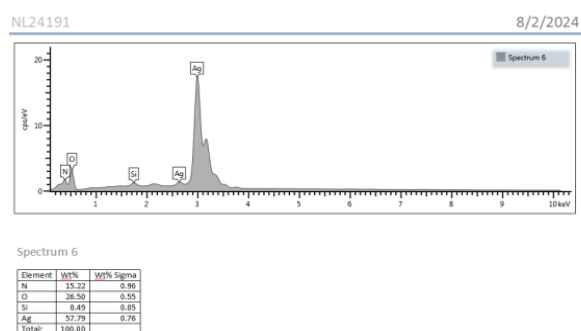


Fig. 8 . EDX spectra analysis of sample 6 .

3.4 . Atomic Force Microscope (AFM) results

The distribution of particle and nanoparticle sizes in dried colloids, prepared as described in (Ag), can be observed. Individual colloids protruding from the slide are visible. Analysis of the representative scan line from the topographic image reveals that protrusions extend from the surface, while height measurements obtained from AFM can be affected by an artifact known as torsion of the specimen. Greater nanoparticle deposits result in larger and more extensive structures. This indicates that nanometer-scale particles move from individual entities on the surface to larger aggregated structures with added nano precipitates. Atomic force microscopy [AFM], operating in air contact mode at room temperature, was used to image the nanoparticles. The AFM images reveal a gravitational interaction between the nanoparticles, resulting in the formation of cohesive aggregates with distinct characteristics, while each nanoparticle maintains its individual properties. The figure illustrates the schematic diagram and particle size distribution of the synthesized AgNPs. The report indicates that the surface roughness , root mean square (rms), and grain size values were measured at [3.67, 4.4 , 65 .79] nm . The schematic diagram depicts the size of the prepared particles.

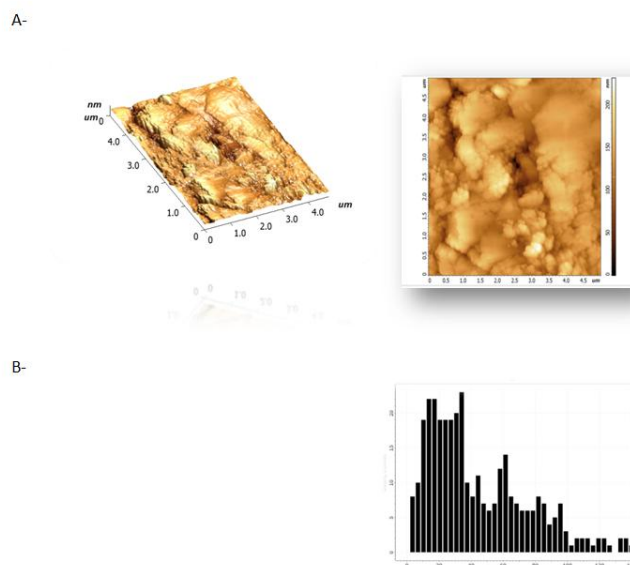


Fig. 9 . AFM image of Sample 1 (A) 2D, 3D, (B) particle size distribution.

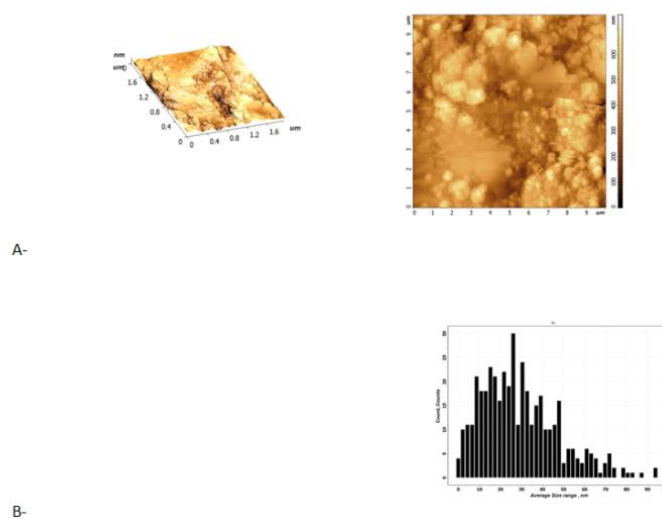


Fig. 10 . AFM image of Sample 2 (A) 2D, 3D, (B) particle size distribution.

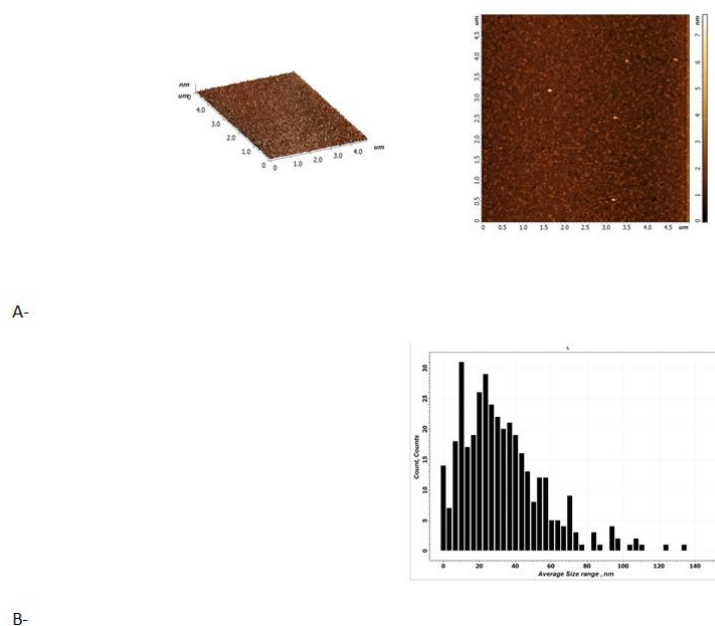


Fig. 11 . AFM image of Sample 3 (A) 2D, 3D, (B) particle size distribution.

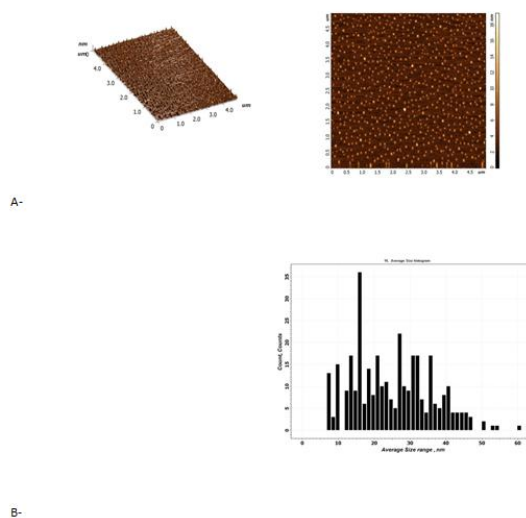
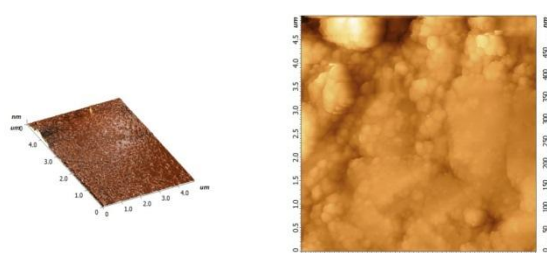
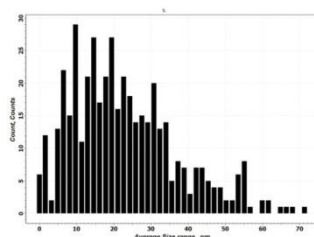


Fig. 12 . AFM image of Sample 4 (A) 2D, 3D, (B) particle size distribution.

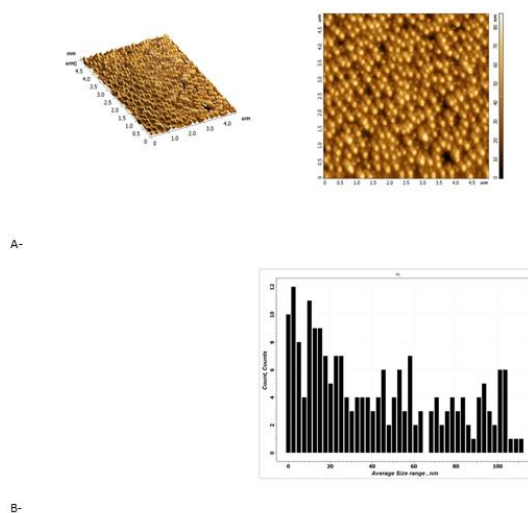


A-



B-

Fig. 13 AFM image of Sample 5 (A) 2D, 3D, (B) particle size distribution.



A-

B-

Fig. 14 AFM image of Sample 6 (A) 2D, 3D, (B) particle size distribution.

Table .1 . Values of surface roughness, mean roughness square [RMS] and particle size of the prepared nanoparticles.

| Sample | Average size (um) | (um) x Grain Size (nm) |
|--------|-------------------|------------------------|
| 1 | 0.066 | 66 |
| 2 | 0.052 | 52 |
| 3 | 0.0539 | 53 |
| 4 | 0.0547 | 54 |
| 5 | 0.0454 | 45 |
| 6 | 0.0666 | 66 |

3.5. Antimicrobial Activity of NPs

The Environmental Research Centre at Technological University in Baghdad, Iraq provided standard isolates

of *Escherichia coli* (25922 ATCC) and *Staphylococcus aureus* (25923 ATCC) for the study. The antimicrobial effects of nanoparticles stem from their physical and chemical interactions with biofilms, which are influenced by the inherent characteristics of nanoparticles including their high surface area-to-volume ratio, distinct particle size, crystalline morphologies (edges and corners), and reactive surface properties [13].studying the effect of Nano materials

Two bacterial isolates were cultured on nutrient agar medium to examine the impact of prepared nano materials on their exteriors. An investigation into the effects of nano materials on bacterial isolates was conducted using the well diffusion method. Silver nanoparticles, at concentrations of [30, 20, 10, 0.0] µg/ml, were used to assess their impact on the growth of Gram-negative *Escherichia coli* bacteria ATCC 25922. The negative charges of *Escherichia coli* and Gram-positive *Staphylococcus aureus* ATCC 25923 were studied for 24 hours at 37°C with constant stirring.

Inhibition Ratio = Test Reading / Control Reading x100 .

Example:

25 = Inhibition zone diameter in the presence of amoxicillin at a concentration of 250 µg/ml .

The nanoparticles [Ag] displayed a significant inhibitory effect, which was found to be dependent on their diameter. The inhibition zone, measured in millimeters, was 0.48 mm for nanoparticles [Ag] at a concentration of 75 µg/ml, as illustrated in Fig 15, and table 2. This demonstrates that the synthesized nano composite [Nystatin/NPs] exhibits similar enhanced properties with regards to its antifungal activity (as indicated in table 3) when compared to the reference [15].

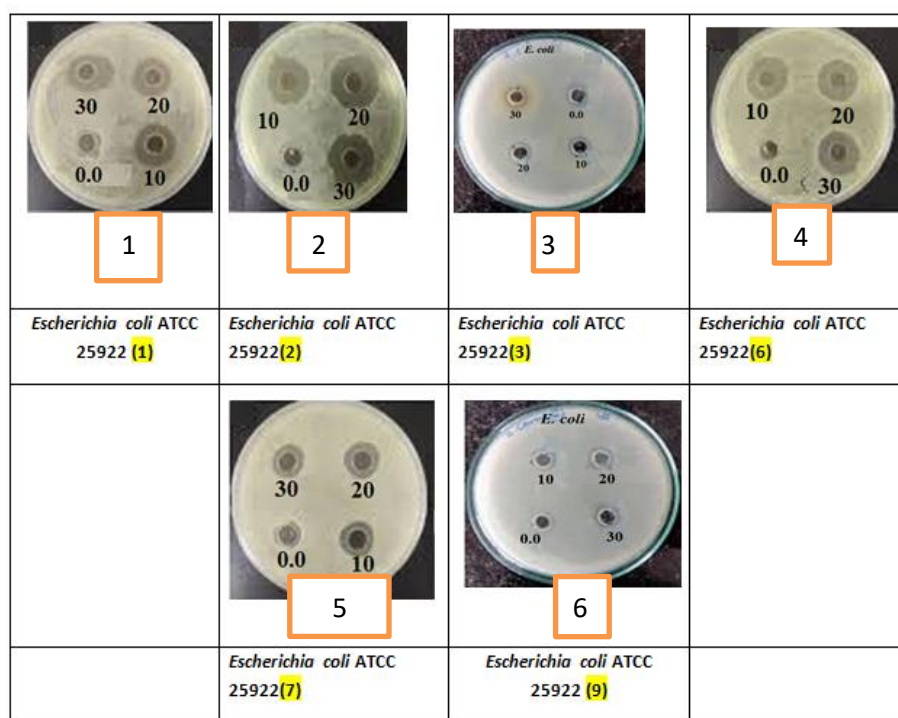


Fig. 15 . shows Zone of inhibition (mm) of gonococci with different concentrations of silver prepared by different methods for *Escherichia coli* ATCC 25922 [17].

Table .2. Inhibition zone diameter [mm] for gonococci with different concentrations of silver prepared by different methods Inhibition zone in [mm] for *Escherichia coli* ATCC 25922.

| Inhibition zone in [mm] | | | | | | |
|------------------------------------|---|---|---|---|---|---|
| <i>Escherichia coli</i> ATCC 25922 | | | | | | |
| Concentration | 1 | 2 | 3 | 4 | 5 | 6 |

| $\mu\text{g/mL}$ | | | | | | |
|------------------|------|------|-----|------|------|------|
| -Ve control | 0.0 | 0.0 | 0.0 | 0.0 | 0.0 | 0.0 |
| 10 | 9.9 | 8.6 | 7.5 | 8.5 | 8.2 | 7.8 |
| 20 | 13.5 | 12.6 | 8.4 | 11.6 | 10.7 | 8.1 |
| 30 | 15.6 | 14.9 | 9.3 | 13.4 | 14.2 | 10.2 |
| +Ve control | 25.6 | | | | | |

Table. 3. Inhibition rate [%] of gonococci with different concentrations of silver prepared by different methods shows the zone of inhibition in mm for *Escherichia coli* ATCC 25922 .

| Inhibition rate [%] | | | | | | |
|------------------------------------|-------|-------|-------|-------|-------|-------|
| <i>Escherichia coli</i> ATCC 25922 | | | | | | |
| Concentration $\mu\text{g/mL}$ | 1 | 2 | 3 | 4 | 5 | 6 |
| -Ve control | 0.0 | 0.0 | 0 | 0.00 | 0.00 | 0.00 |
| 10 | 38.67 | 33.59 | 29.30 | 33.20 | 32.03 | 30.47 |
| 20 | 52.73 | 49.21 | 32.81 | 45.31 | 41.80 | 31.64 |
| 30 | 60.93 | 58.20 | 36.33 | 52.34 | 55.47 | 39.84 |

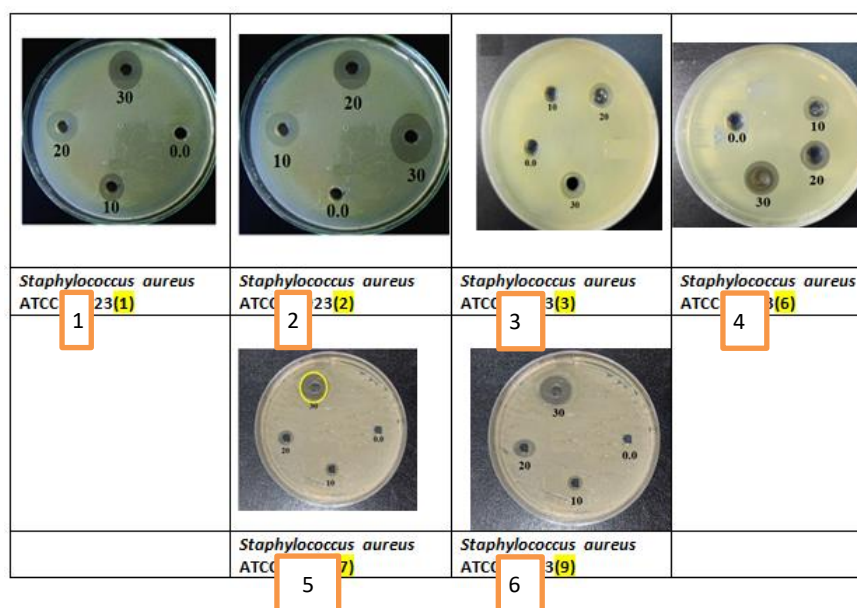


Fig. 16 . Zone of inhibition [mm] of gonococci with different concentrations of silver prepared by different methods for *Staphylococcus aureus* ATCC 25923 .

Table. 4. Inhibition zone diameter [mm] for gonococci with different concentrations of silver prepared by different methods Inhibition zone in [mm] for Staphylococcus aureus ATCC 25923 .

| Inhibition zone in [mm] | | | | | | |
|----------------------------------|------|------|-----|------|------|-----|
| Staphylococcus aureus ATCC 25923 | | | | | | |
| Concentration µg/mL | 1 | 2 | 3 | 4 | 5 | 6 |
| +Ve control | 0.0 | 0.0 | 0.0 | 0.0 | 0.0 | 0.0 |
| 10 | 9.3 | 8.8 | 7.1 | 8.3 | 8.0 | 7.6 |
| 20 | 11.3 | 10.6 | 7.8 | 11.2 | 10.2 | 7.9 |
| 30 | 14.2 | 12.5 | 8.6 | 12.6 | 12.4 | 9.8 |
| +Ve control | 26.8 | | | | | |

Table.5 . Inhibition rate [%] of gonococci with different concentrations of silver prepared by different methods shows the zone of inhibition in mm for Staphylococcus aureus ATCC 25923 .

| Inhibition rate% | | | | | | |
|----------------------------------|-------|-------|-------|-------|-------|-------|
| Staphylococcus aureus ATCC 25923 | | | | | | |
| Concentration µg/mL | 1 | 2 | 3 | 4 | 5 | 6 |
| +Ve control | 34.70 | 0.00 | 0 | 0.00 | 0.00 | 0.00 |
| 10 | 42.16 | 32.84 | 26.49 | 30.97 | 29.85 | 28.36 |
| 20 | 52.99 | 39.55 | 29.10 | 41.79 | 38.06 | 29.48 |
| 30 | 34.70 | 46.64 | 32.09 | 47.01 | 46.27 | 36.57 |

3.6. Antifungal activity of Ag

The study investigated the impact of silver prepared through various methods on the sensitivity and activity of two types of fungi, namely *Trichoaerme*. Harzanium (T.D) and *Apergillus nigar* (A.N) isolated in a dish containing Potato extract agar at a temperature of 34°C. Results from the diffusion method indicated that the prepared nanoparticles exhibited varying degrees of inhibition on the growth of both fungi, with the diameter of the inhibited area increasing with higher concentrations. This observation is supported by fig. 17,18, as referenced in source (18). The solutions utilized at varying concentrations exhibit differences, and an observed trend indicates that the inhibition rate rises with increasing concentrations of silver particles synthesized through various methods. This trend may be attributed to the diminished interactions between Ag and silver in the basic shell structures [19].

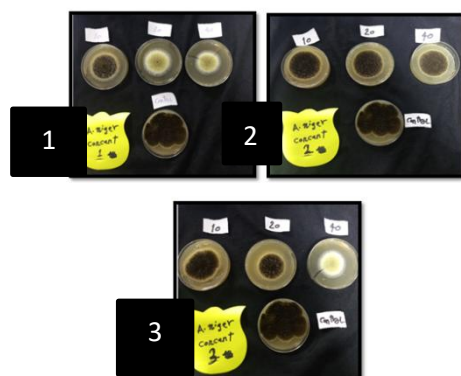


Fig. 17 . Inhibition zone [mm] of fungus [A.N] at different concentrations of silver NPs Prepared in different ways for samples 1, 2, 3.

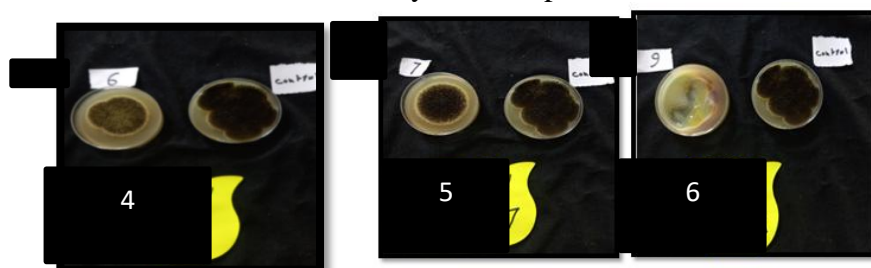


Fig. 18 . Inhibition zone [mm] of fungus [A.N] at different concentrations of silver NPs Prepared in different ways, the last three methods are samples 4, 5, 6.

Table.6 .Diameter of the inhibition zone [mm] for fungi and shows the percentages of inhibition for fungi with different concentrations of silver prepared by different methods for fungi [A.N] ..

| | Inhibition zone in [mm] | | |
|---------------------------|---|---|--|
| [Apergillus. Nigar] [A.N] | A strong fungus with low spread to intestinal infections in water | (A.N)cmx10= [mm] Exempla-5.5cmx10=55mm | Inhibition ratio = test ratio / standard ratio x 100 Exempla- 30÷55X100%=54.54 |
| Concentrati on µg/mL | Ratio concentration[ml] | [A.N] [mm] | Inhibition ratio% |
| Control | 0.0 | 55 | 0.0 |
| 1 | 10 | 43 | 78.18 |
| | 20 | 35 | 63.63 |
| | 40 | 30 | 54.54 |
| 2 | 10 | 45 | 81.81 |
| | 20 | 45 | 81.81 |
| | 40 | 42 | 76.36 |
| 3 | 10 | 50 | 90.90 |
| | 20 | 45 | 81.81 |
| | 40 | 36 | 65.45 |
| 4 | | 40 | 72.72 |
| 5 | | 40 | 72.72 |
| 6 | | No growth | 100% |

Two types of fungi, labeled as [A.N] and [T.D], are present in water. The first type, [A.N], is known for causing intestinal infections and exhibits strong but limited spreading characteristics. In contrast, the second type, [T.D], has weaker spreading capabilities but is more widespread and rapid in its spread within water sources. In an experimental setting, the inhibition of both types of fungi is evident through visual representations with corresponding percentage values displayed in a table. The inhibition rates for the second type decrease gradually over time when subjected to concentrations of 40 and 20, indicating slow or minimal efficacy. Furthermore, it is observed that sample 6 experiences significant fungal fatality due to exposure to silver nitrate under acidic conditions ($\text{pH} < 7$), demonstrating the detrimental impact of nitrate on both types of fungi. The data illustrates that inhibition is influenced by the concentration of nanomaterial as well as the properties of the medium, particularly when it is acidic. This suggests that an acidic medium may not be suitable for fungal growth.



Fig. 19 .Inhibition zone [mm] of fungus [T.D] at different concentrations of silver NPs Prepared in different ways for samples 1,2,3 .

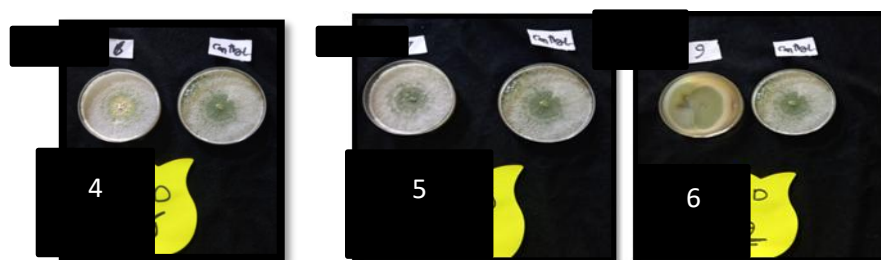


Fig. 20 . Inhibition zone [mm] of fungus [T.D] at different concentrations of silver NPs Prepared in different ways, the last three methods samples 4,5,6 .

The pH level also plays a significant role. In environments with a pH below 7, it acts as an inhibitor, suppressing the growth of fungi and bacteria, rendering the environment inhospitable to them. The two types of fungi, [A.N] and [T.D], are found in water. [A.N] is a type that spreads weakly but is potent in causing intestinal infections, while [T.D] is a widely spreading and fast-spreading type. The inhibition of both types of fungi is clearly depicted in the accompanying images, with the inhibition percentage presented in the table 7. At concentrations of 40 and 20, the inhibition rate for [T.D] is (41.81) which decreases at levels. Samples 1,2, 3, 4, and 5,6 and fig 19,20 shows inhibition of fungal growth. demonstrates that silver nitrate and acidic pH levels are fatal to both types of fungi. The inhibition rates are influenced by the concentration of nanomaterial and the nature of the medium. In acidic conditions, fungal growth is inhibited, rendering the medium unsuitable for their development. The pH level of the environment also plays a significant role. When the pH is below 7, it acts as an inhibitor for fungi and diminishes their growth, consequently creating an inhospitable environment for both fungi and bacteria.

Table.7. Diameter of the zone of inhibition [mm] for type 2 fungi. It shows the percentages of inhibition for the fungus with different concentrations of silver prepared by different methods for the fungus [T.D].

| | Inhibition zone in [mm] | | |
|-------------------------------|--|--|--|
| [Trichoerme. Harzanium] [T.D] | Weak, highly pathogenic fungi for intestinal infections found in water | [T.D]cmx10= [mm] Exmpal- 5.5cmx10=55mm | Inhibition ratio = test ratio / standard ratio x 100 Exempla- 30÷55X100%=54.54 |
| Concentration µg/mL | Ratio concentration(ml) | [T.D] [mm] | Inhibition ratio% |
| Control | 0.0 | 55 | 0.0 |
| 1 | 10 | Heavy | 0 |
| | 20 | 50 | 90.90 |
| | 40 | 23 | 41.81 |
| 2 | 10 | Heavy | 0 |
| | 20 | Heavy | 0 |
| | 40 | Heavy | 0 |
| 3 | 10 | Heavy | 0 |
| | 20 | Heavy | 0 |
| | 40 | 37 | 67.27 |
| 4 | | Heavy | 0 |
| 5 | | Heavy | 0 |
| 6 | | No growth | 100% |

4-CONCLUSIONS

Silver powders and liquids, when prepared as samples, have been found to be effective in inhibiting the growth of bacteria and fungi. They have been used to inhibit the growth of water-polluting bacteria, and two types of bacteria and two types of fungi were taken. The inhibition rate of nanosilver on bacteria increases with the smaller diameters of the prepared nanosize and the longer the exposure period. Nanosilver is important in water purification because it acts as an inhibitor of microorganisms. Tests conducted prove that nanosilver exists, and its effectiveness in inhibiting bacteria and fungi varies depending on the method of preparation, with smaller particles being more effective in killing microorganisms .

AKNOWLEDGEMENTS

I would like to thank the supervisors who helped me and thank everyone who helped me write the research and thank the editor-in-chief of your journal for receiving the research .

5-REFERENCES

1. Karaneh Eftekhari¹ ., K.Mehraj Pasha² ., Sanjeeva Prasad Tarigopula³ ., Mounica Sura⁴ ., Jayasimha Rayalu Daddam^{5*}. BIOSYNTHESIS AND CHARACTERIZATION OF SILVER AND IRON NANOPARTICLES FROM SPINACIA OLERACEA AND THEIR ANTIMICROBIAL STUDIES. Volume-5, Issue-1, Jan-Mar,(2015) .
2. Siddique-Ur-Rahman, Kishwar Sultana & Muhammad Tauseef Qureshi . GREEN SYNTHESIS OF SILVER NANO PARTICLES USING SPINACIA OLERACEA LEAVE EXTRACT AND THEIR PHYSICAL VERIFICATION . Article • January, (2017).
<https://www.researchgate.net/publication/349964238>.

3. Abdullah Abdul Karim Hassan and Saif Saad Allah Hassan. Evaluation of the efficiency of silver nanoparticles prepared biologically from mushroom food. Syrian Journal of Agricultural Research 8(6): 348-357 December , (2021).
4. Helinor J. Johnston^{1,2}, Gary Hutchison¹ , Frans M. Christensen³ , Sheona Peters⁴ , Steve Hankin⁴ , and Vicki Stone¹ . A review of the in vivo and in vitro toxicity of silver and gold particulates: Particle attributes and biological mechanisms responsible for the observed toxicity . Critical Reviews in Toxicology; 40(4): 328–346, (2010) .
5. Ahmed T El-Aref . Silver nanoparticles: preparation, characterization, cytotoxicity, and its impact on cotton fabrics . Architecture and Arts Magazine, Issue Thirteen ,(2018). DOI: 10.21608/mjaf.(2018) .
6. Ayed Al-Qurashi Nebula ,Ahmed Ibrahim Al-Saqqaf , Jazem Abdullah Mahyoub . Biological effects of silver nanoparticles prepared from extract Thevetia neriifolia plant against L. pipiens Culex mosquito larvae. JKAU: Sci., Vol. 27. No 2 pp: 13-23, (2015) . DOI:10.4197/Sci.27-1.3 .
7. Amir Reda Sadr al-Husseini, Muhammad Adzir Mahdi, Farida Alizadeh and Soraya Abdel Rashid. Laser ablation technology for metal synthesis Nanoparticles in liquid,(2018). <http://dx.doi.org/10.5772/intechopen.80374>
8. Marta Paszkiewicz,¹ Anna GoBdbiewska,² Aukasz Rajski,³ Ewelina Kowal,³ Agnieszka Sajdak,³ and Adriana Zaleska-Medynska¹ . Synthesis and Characterization of Monometallic (Ag, Cu) and Bimetallic Ag-Cu Particles for Antibacterial and Antifungal Applications . Hindawi Publishing Corporation Journal of Nanomaterials Volume 2016, Article ID 2187940, 11 pages ,(2016). <http://dx.doi.org/10.1155/2016/2187940>
9. Ghaith Abdul Zahra Jawad. Biosynthesis of silver nanogels. Department of Chemistry, College of Education,(2018).
10. Jassim Younis Jassim Al-Obaidi . Evaluation of the role of silver nanoparticles manufactured by Pomegranate peel extract against Aspergillus mold And the pathological effects of Afla toxin B on broiler chickens. Master's thesis Veterinary Medicine/Poultry Diseases, University of Mosul,(2022)
11. Raghad Zein 1,* , Ibrahim Alghoraibi 1,2 , Chadi Soukkarieh 3 and Abdalrahim Alahmad 4,* Investigation of Cytotoxicity of Bio synthesized Colloidal Nanosilver against Local Leishmania tropica: In Vitro Study . Materials, 15, 4880 ,(2022). <https://doi.org/10.3390/ma15144880> <https://www.mdpi.com/journal/materials>
12. Liliana Marinescu , 1 Denisa Ficai , 1 Ovidiu Oprea , 1 Alexandru Marin , 2 Anton Ficai , 1,3 Ecaterina Andronesco , 1,3and Alina-Maria Holban 4. Optimized Synthesis Approaches of Metal Nanoparticles with Antimicrobial Applications. Hindawi Journal of Nanomaterials Volume 2020, Article ID 6651207, 14 pages ,(2020) . <https://doi.org/10.1155/2020/6651207>
13. Chukwuebuka Egbuna , 1,2,3 Vijaykumar K. Parmar,⁴ Jaison Jeevanandam,⁵. Toxicity of Nanoparticles in Biomedical Application: Nanotoxicology . Hindawi Journal of Toxicology Volume ,(2021). Article ID 9954443, 21 pages .2021. <https://doi.org/10.1155/2021/9954443> .
14. A. K. Gade¹, P. Bonde¹, A. P. Ingle¹, P. D. Marcato², N. Durán^{2 3}, and M. K. Rai^{1 *} .Exploitation of Aspergillus Niger for Synthesis of Silver Nanoparticles . Journal of Biobased Materials and Bioenergy Vol.2, 1–5, (2008) .
15. Samer Hasan Hussein-Al-Ali,^{1,2} Mohamed E. El Zowalaty,^{3,4} Aminu Umar Kura,⁴ Benjamin Geilich,⁵ Sharida Fakurazi,^{4,6} Thomas J. Webster,^{5,7} and Mohd Zobir Hussein⁸ . Antimicrobial and Controlled Release Studies of a Novel Nystatin Conjugated Iron Oxide Nanocomposite . Hindawi Publishing Corporation BioMed Research International Volume, Article ID 651831, 13 pages ,(2014) . <http://dx.doi.org/10.1155/2014/651831>
16. Salma Salman Abdullah . Preparation of (Au, Ag, Ti and Cu) Nanoparticles by Pulsed Laser Ablation in Liquid (PLAL) Technique for Medical Applications . University of Diyala College of Science Department of Physics,(2022) .
17. Amany A. El-Kheshen^{1,2*} and Sanaa F. Gad El-Rab^{1,3} . Effect of reducing and protecting agents on size of silver nanoparticles and their anti-bacterial activity . Der Pharma Chemica, , 4 (1):53-65,(2012) .<http://derpharmachemica.com/archive.html> .

18. Kristian Fog Nielsen & Jesper Mølgaard Mogensen & Maria Johansen & Thomas O. Larsen & Jens Christian Frisvad . Review of secondary metabolites and mycotoxins from the *Aspergillus niger* group . *Anal Bioanal Chem* 395:1225–1242 ,(2009). DOI 10.1007/s00216-009-3081-5 .
19. Margo A. Kusters-van Someren, Jan A.M. Harmsen*, Harry C.M. Kester, and Jaap Visser . Structure of the *Aspergillus niger* *peA* gene and its expression in *Aspergillus niger* and *Aspergillus nidulans* . *Curt Genet* 20:293-299 , (1991).
20. Shaimaa Obaid Hasson¹ , Mohammed Jabber Al-Awady² , Adnan Hamad Al-Hamadani³ , Ibtisam Habeeb Al-Azawi³ , Alaa Irhayyim Ali . Boosting Antimicrobial Activity of Imipenem in Combination with Silver Nanoparticles towards *S. fonticola* and *Pantoea* sp.. 11(2): 200-214. (2019) .doi: 10.5101/nbe.v11i2.p200-214